



An Artificial Magnetic
Conductor (AMC) Operating in the Band
7.51-15.24 GHz

Zhang Qichen, Zhu Wuyingshu and Guan Yalin

EasyChair preprints are intended for rapid dissemination of research results and are integrated with the rest of EasyChair.

July 6, 2020

A Artificial magnetic conductor (AMC) operating in the band 7.51-15.24 GHz

Qichen Zhang

School of Information Engineering
Communication University of China
Beijing, China
zhangqichen1997@outlook.com

Wuyingshu Zhu

School of Information Engineering
Communication University of China
Beijing, China
zhuwuyingshuz@163.com

Yalin Guan

School of Information Engineering
Communication University of China
Beijing, China

Abstract—In this paper, a 50×50 unit composed of artificial magnetic conductor (AMC), works on the frequency band of 7.51-15.24 GHz and the bandwidth reaches 67.96% is proposed. The designed structure has the advantages of small size, wide bandwidth, easy processing, stable performance, and low sensitivity. The presented AMC is simulated, fabricated and measured. The measured results are in good agreement with the simulated ones. The size of the three-dimensional artificial magnetic conductor unit is $6\text{mm} \times 6\text{mm} \times 4\text{mm}$.

Keywords—Artificial magnetic conductor (AMC), reflected phase, broadband FSS, Equivalent Circuit.

I. INTRODUCTION

As an electromagnetic metamaterial, the artificial magnetic conductor (AMC) structure has ideal magnetic surface characteristics in a special frequency band, and can break through the structural limit of the conventional antenna in the design of the antenna. However, the typical planar patch-type AMC structure is difficult to break through in low frequency, miniaturization, and wideband. Therefore, the research on the broadband stereo AMC structure developed in the vertical direction meets the actual needs.

Based on the mushroom-type AMC structure proposed by D. Sievenpiper, researchers and scholars have conducted in-depth research on it, and proposed an equivalent circuit model for analyzing the phase characteristics of reflection, and found the relationship between the zero-point phase reflection point and its operating frequency. In 2014, Rayno J et al. proposed a 3D AMC structure for gene programming, but the internal structure of the design is complex and not regular, and the actual processing is difficult.

In this paper, a wide-range $6\text{mm} \times 6\text{mm} \times 4\text{mm}$ three-dimensional artificial magnetic conductor unit is proposed. An artificial magnetic conductor composed of 50×50 units was developed. The simulation proves that the broadband AMC structure can work in the 7.51-15.24 GHz band, and the bandwidth can reach 67.96%. It has many advantages such as small size, wide bandwidth, easy processing and low sensitivity.

II. THEORY IN AMC DESIGN

Take the classic mushroom type AMC as an example, the Schematic diagram of plane wave incident of AMC structure in Fig.1. Assuming that the YOZ plane is a high impedance surface, the incident wave propagates negatively along the x-axis.

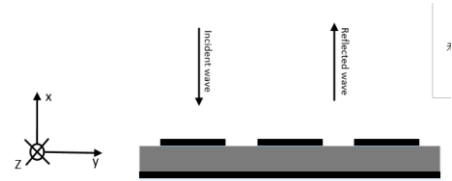


Fig. 1. Equivalent circuit model of AMC structure

Usually we define a region with a reflection phase between $+90^\circ$ and -90° as the in-phase reflection region. From reference [10], the ratio of the frequency range of the in-phase reflection zone to the center frequency is defined as the relative bandwidth of the artificial magnetic conductor, which is expressed as follows:

$$BW = \frac{f_H - f_L}{f_0} \times 100\% \quad (1)$$

The in-phase reflection characteristics of the AMC structure are similar to those of an ideal magnetic conductor. Therefore, the AMC structure can be used as a reflector of the horizontal antenna, so that the antenna can be placed close to the AMC surface, thereby achieving the purpose of reducing the height of the antenna.

III. THE STRUCTURES OF AMC

Broadband stereo AMC unit structure is shown in Fig. 2. It consists of two dielectric plates, two rectangular open annular patches and metal vias. By discussing the shape of the patch, the position of the patch in the medium, the location of the via, and the extent of the penetration of the via to the reflection phase bandwidth, the design is optimized to determine the appropriate parameters. The thickness of the upper and lower layers is 2mm, the length and width of the medium are 6mm, the length and width of the rectangular annular metal patch are 2mm, the through hole is tangent to the three sides of the opening of the rectangular ring, the diameter is 0.5mm, and the width of the rectangular ring is wide. It is 0.6mm. Two rectangular annular patches are divided into upper surfaces of the upper and lower layers and connected by via holes.

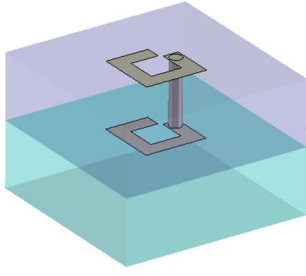


Fig. 2. Broadband stereo AMC unit structure

Broad-band stereo AMC structural unit top view (a) and side view (b), The patch is centered on the top surface of the media. The width of the patch is equal to the diameter of the via, so the via is just tangent to the three sides of the patch opening.

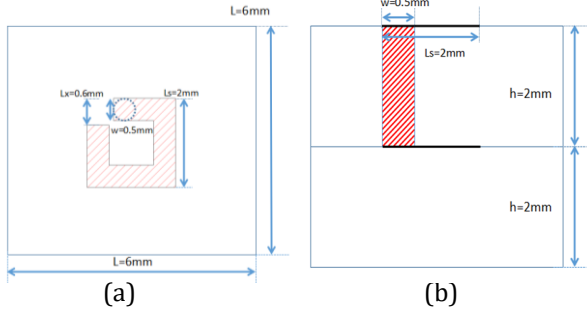


Fig. 3. Broad-band stereo AMC structural unit top view (a) and side view (b)

For a single-layer artificial magnetic conductor structure, it can be equivalent to a parallel LC loop. By equivalent circuit analysis method similar to the single-layer artificial magnetic conductor structure, we can build the equivalent circuit of the three-dimensional artificial magnetic conductor shown in Fig. 4. Fig.5 is shown the Schematic diagram of equivalent circuit of three-dimensional artificial magnetic conductor. Model for the three-dimensional AMC structure, the upper and lower layers can equivalent to the parallel LC circuit, and then the upper and lower layers of the LC circuit are connected in parallel, that is equivalent to the two-stage parallel oscillating circuit of the capacitor and inductor. The capacitance values of the upper layer and the lower layer are different, and the inductance values provided by the vias are also different. The gap between adjacent metal patches on each layer provides capacitance and the inductance is determined by the thickness and permeability of each substrate

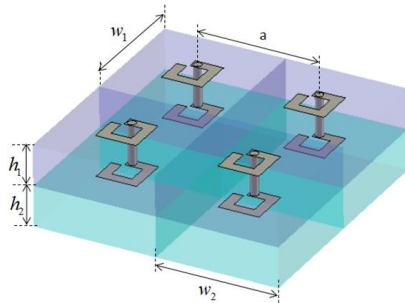


Fig. 4. Schematic diagram of three-dimensional artificial magnetic conductor structure

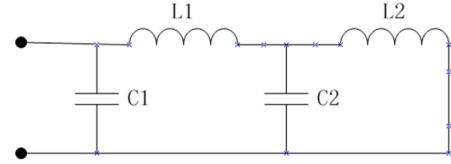


Fig. 5. Schematic diagram of equivalent circuit of three-dimensional artificial magnetic conductor

IV. ANALYZE

The AMC structure was simulated by HFSS. The comparison of reflection phase of equivalent circuit and modeling simulation in Fig.6. The simulation results show that the overall trend of the two curves is consistent and almost coincides in the operating band of 7.51-11.24 GHz. The resonance point and bandwidth error are all within an acceptable range. The comparison chart proves that the equivalent circuit we built has certain reliability. The specific values of the comparison are shown in Table 1.

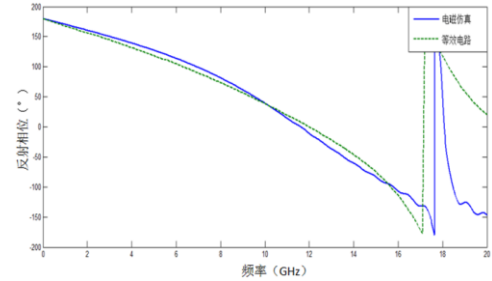


Fig. 6. Comparison of reflection phase of equivalent circuit and modeling simulation

表 4.1 电磁仿真与等效电路反射相位对比

Calculation	$f_{\phi} = 90^{\circ}$	$f_{\phi} = 0^{\circ}$	$f_{\phi} = -90^{\circ}$	Relative bandwidth
Equivalent Circuit	6.95	11.95	15.40	75.62%
simulation	7.51	11.6	15.24	67.96%

In order to ensure that the machining error has no influence on the performance of the designed artificial magnetic conductor structure, the thickness of the dielectric plate, the side length of the patch and the error of the via diameter may be analyzed before processing. When the thickness of single-layer dielectric plate of F4BM-365 material is 2mm, the tolerance is $\pm 0.05 \sim \pm 0.07$ mm, and the thickness of two-layer dielectric plate is 4mm, the error may be $\pm 0.1 \sim \pm 0.14$. For the convenience of calculation, we can follow the maximum error that may occur. An approximation of 0.1 mm was used for analysis. That is, the thickness h of the single-layer dielectric plate dielectric plate is 1.9mm, 2.0mm, 2.1mm for error analysis, and the simulated reflection phase and reflection amplitude are as shown in Fig. 7(a). The side length of the patch is 2mm, and the single-layer dielectric plate The thickness is consistent, and we also assume an error of ± 0.1 mm for analysis when doing machining error analysis. That is, ls are taken as 1.9mm, 2.0mm, 2.1mm respectively, and their simulation results are shown in Fig. 7(b). The vias penetrate from the upper surface of the first layer of media to the upper surface of the second layer of media, i.e., just the vias connect the upper and lower metal patches. The via diameter is 0.5mm, which is tangent to the patch. In

order to ensure that the via process error does not have much influence on the reflection phase of the structure, the error is $\pm 0.1\text{mm}$, and the simulation result is shown in Fig.7(c).

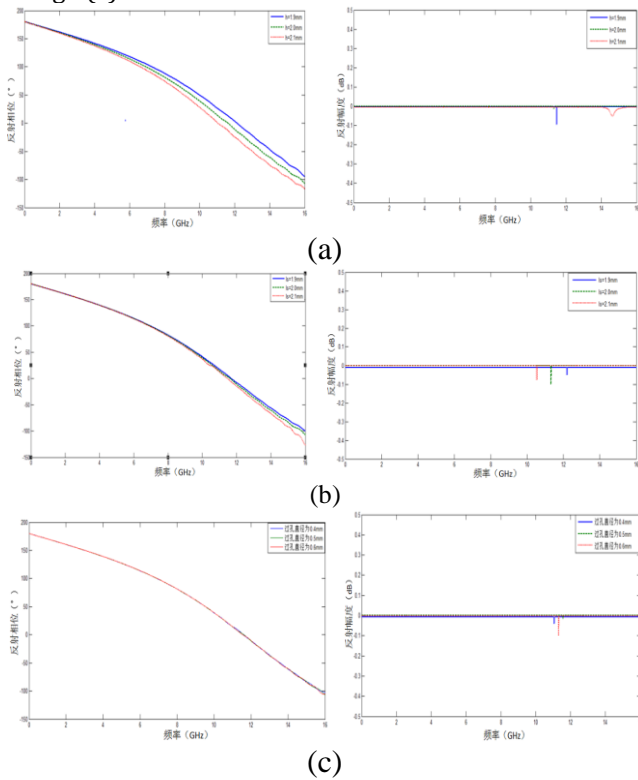


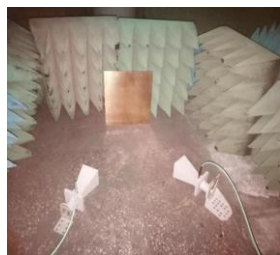
Fig. 7. Reflection phase and reflection amplitude versus frequency

It can be seen from the figure that the three parameters of the reflection phase and the reflection amplitude are basically coincident in the error range of 0.1 mm, which proves that the designed structure in this range is stable and is not affected by the process error.

The processed AMC structure upper and lower dielectric plates are all made of F4BM-365 material, and the processed objects are shown in Figure 8(a). They are divided into three layers. The upper layer and the middle layer structure are basically the same, and the bottom layer is copper-clad metal plate. The board size is 300mm 300mm. The two horn antennas covering the 7-15 GHz operating frequency and the test board form an isosceles right triangle. One horn antenna is used as the transmitting antenna, and the other is used as the receiving antenna for testing. The antennas are respectively connected to the output and input ports of the vector network analyzer. As shown in Fig.8(b), the reflection phase of the AMC surface is first measured, and then the metal plates of the same size are placed at the same position, and the reflection phase is measured for calibration.



(a)



(b)

Fig. 8. Broadband stereo AMC physical map
Since the design of the board is a large size, the space wave test method is adopted and the TRL calibration method is selected. The calibration result is shown in Fig. 9.

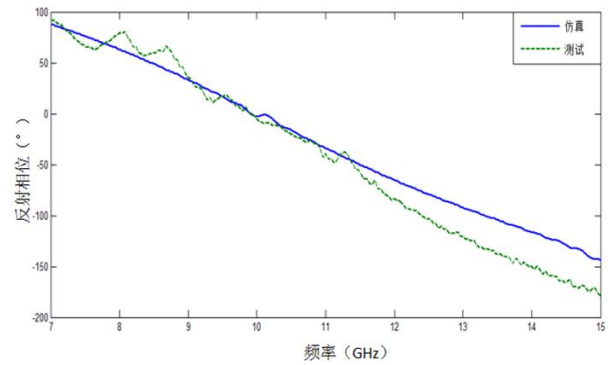


Fig. 9. Physical test and electromagnetic simulation reflection phase comparison chart

CONCLUSION

This paper proposes a wideband 6mm 6mm 4mm three-dimensional AMC structural unit. It can operate in the 7.51-15.24 GHz band with a bandwidth of 67.96%. From the simulation results, the influence of the thickness of the dielectric plate, the error of the side length of the patch and the diameter of the via on the reflection phase and the reflection amplitude are analyzed. The processed material meets the expected requirements.

ACKNOWLEDGMENT

REFERENCES

- [1] Z.W.Ma. "The Research on Microwave Dual-Band Bandpass Filters for Wireless Communication", Shanghai University, 20106.
- [2] Y. Liu, Y.S. .Dai, DC.Qiao. "A Design of Dual-band Band-pass Filter with Miniaturization Based on LTCC Technology" in 2016 IEEE International Conference on Microwave and Millimeter Wave Technology (ICMMT), 2016, pp: 333-335.
- [3] J.X.Xu and X.Y.Zhang. "Single and Dual-Band LTCC Filtering Switch With High Isolation Based on Coupling Control" in IEEE Transactions on Industrial Electronics, *J. Magn.*, vol. 64, pp. 3137-3146, 2017.
- [4] L.C.Tsai, C.W.Hsue. "Dual-Band Bandpass Filters Using Equal-Length Coupled-Serial-Shunted Lines and Z-Transform Technique" in IEEE Transactions on Microwave Theory And Techniques, *J. Magn.*, vol. 52, pp. 1111-1117, 2004.
- [5] M.Sagawa, M.Makimoto, S.Yamashita. "Geometrical Structures and Fundamental Characteristics of Microwave Stepped-Impedance Resonators" in IEEE Transactions on Microwave Theory and Techniques, *J. Magn.*, vol. 45, pp. 1078-1085, 1997.
- [6] C.W.Tang, H.C.Hsu, J.W.Wu. "Design of a LTCC Dual-Passband Filter With Stepped Impedance Resonators" in Proceedings of Asia-Pacific Microwave Conference, 2007, pp. 1- 4.
- [7] X.Dai, X.Y.Zhang, Z.Y.Cai. "Compact LTCC Dual-Band Bandpass Filter Using Stepped Impedance Resonators" in 2013 Cross Strait Quad-Regional Radio Science and Wireless Technology Conference, 2013, pp. 109-112.
- [8] H.Clark Bell. "Zolotarev Bandpass Filters" in IEEE Transactions on Microwave Theory and Techniques, *J. Magn.*, vol. 49, pp. 2357-2362, 2001.
- [9] S.Sun, L.Zhu. "Compact Dual-Band Microstrip Bandpass Filter Without External Feeds" in IEEE Microwave And Wireless Components Letters, *J. Magn.*, vol. 15, pp. 644-646, 2005.
- [10] H.Wang. "Theory and Realization of Controllable Mixed Electric and Magnetic Coupling Filters", South China University of Technology, 2010.